The tuning approach proposed to adjust the poles' positions consists in slightly varying the length of only one resonator. Figure 10 illustrates its effect on the resonance frequencies. It can be seen from Figure 10 that if the length of only one resonator varies slightly, the corresponding resonance peak shifts by a considerable amount, as compared to the smaller shift in the other resonance peak. In this case, it is possible to enhance a given performance of the filter without considerably affecting the others since only one pole is shifted. In such conditions, the poles' positions can be easily corrected to enhance filter performance. This technique allows the improvement of results in terms of frequency response for both the return loss and the ripple level. By using this tuning technique, the first prototype was optimized. The dimensions of the optimized prototype can be found in Table 1 (see second line). It can be noted from Table 1 that two resonators have been extended by 0.1 mm and two others by 0.2 mm, while the spacing between the different resonators have been kept unchanged. Figure 11 gives the simulated frequency responses. As predicted, this tuning technique provides a high potential for redressing various filter performances. It is noted from the curve shown in Figure 11 that a very considerable enhancement in terms of the return loss is achieved by using this tuning technique. The maximum S_{11} obtained along the entire passband is -20 dB, which represents more than 10-dB enhancement. The ripple level has also been improved and the variation of 10^{-2} dB represents an enhancement of 1 dB. To validate our approach, the filter has been implemented and tested.

5. EXPERIMENTAL RESULTS

The optimized filter has been designed and constructed on a duroid substrate with a dielectric constant ε_r of 3.38 and thickness of 0.81 mm. Figure 12 shows the photograph of the fabricated filter.

After tuning, the fabricated filter was measured using an HP8719 network analyzer. Figure 13 plots the measured frequency responses of the tuned filter. The filter has a center frequency of 2.14 GHz and a passband from 2.11 GHz to 2.17 GHz. It is important to mention that the choice of the filter passband was made so that this filter could be used for wireless applications such as PCS systems of the third generation. It can be noted form these curves that the experimental results give a good agreement with the numerical ones. The maximum measured value of S_{11} along the entire passband is -15 dB, which represents a sufficient match performance. However, the simulations do not include conductor loss, and a difference of 3 dB in the insertion loss is seen between the numerical and experimental results. The measured bandwidth and the ripple level correspond well to simulation results.

6. CONCLUSION

The design of a miniaturized microstrip cross-coupled resonator filter has been developed. A high level of miniaturization was achieved by considering the problem at the overall filter level and the resonator level. To solve the problem of filter mismatch, a new tuning technique to redress return loss without deteriorating the overall filter performance has also been introduced. This approach requires only a slight modification of the length of some resonators. With this technique, even if the filter is printed on the substrate, it still possible to be tuned. Simulations and measurements were performed and the results indicated that this filter design is simple, practical, and effective for achieving excellent performance. The proposed filter design is suitable for wireless and mobile communications applications.

REFERENCES

1. K.C. Gupta, R. Garg, and I.J. Bahl, Microstrip lines and slot lines, 2nd ed., Artech House, Norwood, MA, 1996.
2. H. Howe, Stripline Circuit Design, Artech House, Norwood, MA, 1974.
3. G.L. Matthaei, L. Young, and E.M.T. Jones, Microwave filters, impedance-matching networks, and coupling structures, 2nd ed., Artech House, Norwood, MA, 1985.
4. ADS manual, Agilent Technologies, Santa Rosa, CA, 2000.
5. M. Makimoto, Microstrip-line split-ring resonators and their application to bandpass filters, Electron Commun 72 (1989), 104–113.
6. J.S. Wong, Microstrip tapped-line filter design, IEEE Trans Microwave Theory Techniques 27 (1979), 44–50.
7. M. Sagawa, K. Takahashi, and M. Makimoto, Miniaturized hairpin resonators filters and their application to receiver front-end MIC's, IEEE Trans Microwave Theory Techniques 37 (1989), 1991–1996.
8. J. Hong and M.J. Lancaster, Coupling of microstrip square open-loop resonators for cross-coupled planar microwave filters, IEEE Trans Microwave Theory Techniques 44 (1996), 2099–2109.
9. J. Hong and M.J. Lancaster, Cross-coupled microstrip hairpin-resonator filters, IEEE Trans Microwave Theory Techniques 46 (1998), 118–122.
10. S. Darlington, Synthesis of reactance four poles which produce prescribed insertion loss characteristics, J Math Phys 18 (1939), 257–353.
11. R. Levy, Filters with single transmission zero at real or imaginary frequencies, IEEE Trans Microwave Theory Techniques 24 (1976), 172–181.
12. M. Makimoto and M. Sagawa, Varactor tuned bandpass filters using microstrip-line ring resonators, IEEE MTT Symp Dig (1986), 411–414.
13. M. Sagawa, I. Ishigaki, M. Makimoto, and T. Naruse, Dielectric split-ring resonators and their applications to filters and oscillators, IEEE MTT-S Symp Dig (1988), 605–608.
14. ENSEMBLE, Design User's Guide, Ansoft, USA, 1998.

PRINTED ANTENNA DESIGN FOR BROADBAND WAVEGUIDE-BASED SPATIAL POWER COMBINERS

Milan V. Lukic,[1] Alexander B. Yakovlev,[1] Atef Z. Elsherbeni,[1] Charles E. Smith,[1] and Michael B. Steer[2]
[1] Department of Electrical Engineering
University of Mississippi
University, MS 38677-1848
[2] Department of Electrical and Computer Engineering
North Carolina State University
Raleigh, NC 27695-7914

Received 14 August 2002

ABSTRACT: *Design of broadband printed antennas, including the finite arrays of interacting patch, U-strip, U-slot, and meander slot antennas, are presented for applications in waveguide-based spatial power combiners operating at X-band. The effect of several antenna design parameters on antenna bandwidth performance is investigated in this paper. The antenna designs presented show significant advantages in their scattering characteristics compared to rectangular patch and slot antennas traditionally used in spatial power combiners.* © 2003 Wiley Periodicals, Inc. Microwave Opt Technol Lett 36: 411–415, 2003; Published online in Wiley InterScience (www.interscience.wiley.com). DOI 10.1002/mop.10778

Key words: *spatial power combining; meander-slot antenna; U-slot antenna; antenna array*

1. INTRODUCTION

To exploit the advantages of solid-state technology for high power levels at microwave and millimeter-wave frequencies, the power from many individual devices must be combined because of the fundamental limits of semiconductor devices' power-handling capability at these frequencies [1]. Spatial power combining (SPC) techniques provide high combining efficiency for high power levels in microwave and millimeter-wave regimes, using free space rather than waveguide and transmission line junctions originally introduced in circuit-combining structures. These techniques have been applied to oscillators, amplifiers, mixers, phase-shifters, switches, frequency multipliers, and modulators. Recently, a review of quasi-optical array systems operating in the microwave and millimeter-wave regime, with a focus on power amplifiers, was presented in [1].

From the modeling point of view, spatial power combiners are very complex systems and cannot be entirely modeled and designed using any of the commercially available general-purpose electromagnetic (EM) CAD tools. Instead, a customized EM analysis needs to be developed for their characterization and design [2–9]. A method of moments (MoM) based generalized scattering matrix (GSM) modeling environment for efficient simulation of large waveguide EM and quasi-optical systems for SPC has been developed in [5–9]. The EM modeling scheme is based on the decomposition of the system into individual modules (blocks) and calculation of the GSM of each module using the most convenient technique. The GSMs of each block are then cascaded to obtain the overall system characterization. The work presented in [5] focuses on efficient formulation of the GSM for a single arbitrarily shaped planar conductive layer in a shielded guided-wave structure. The MoM formulation implemented in [7] enables the incorporation of the EM model of a microwave structure into a nonlinear microwave-circuit simulator as required in global CAD. In [8], a full-wave integral-equation formulation is developed for the EM modeling of waveguide-based, closely-spaced electric and magnetic discontinuities. A full-wave analysis and experimental validation of a waveguide-based aperture-coupled patch amplifier array is presented in [9]. Here, a GSM for an N-port waveguide transition containing an aperture-coupled patch array is developed using the procedure presented in [8] for the two-port waveguide transition.

In this paper, we present a waveguide transition consisting of several interacting printed antenna arrays placed at dielectric interfaces of an oversized multilayered waveguide (Fig. 1). This passive antenna module serves as an integral part of waveguide-based amplifier arrays (for example, the aperture-coupled patch antenna array presented in [9]). Narrowband resonant rectangular patch and slot antennas used in earlier designs [8, 9] are replaced by meander-slot antennas and their modifications [10, 11], in order to increase the frequency bandwidth and efficiency of the system. Numerical results are presented for the interacting single patch and meander slot antennas as well as finite arrays of interacting U-strip, U-slot, and meander slot antennas, illustrating advantages of their utilization in a waveguide-based power combining system.

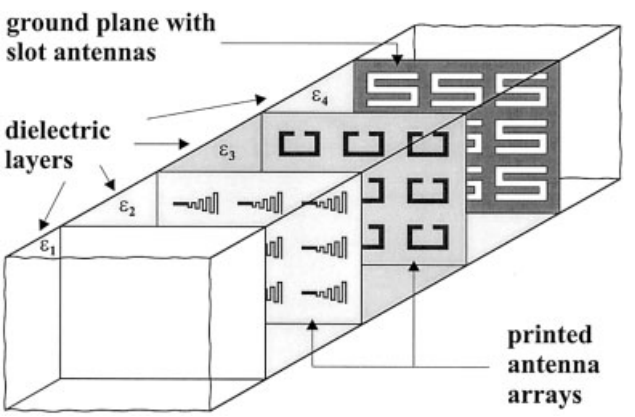

Figure 1 Multilayered waveguide transition containing interacting printed antenna arrays

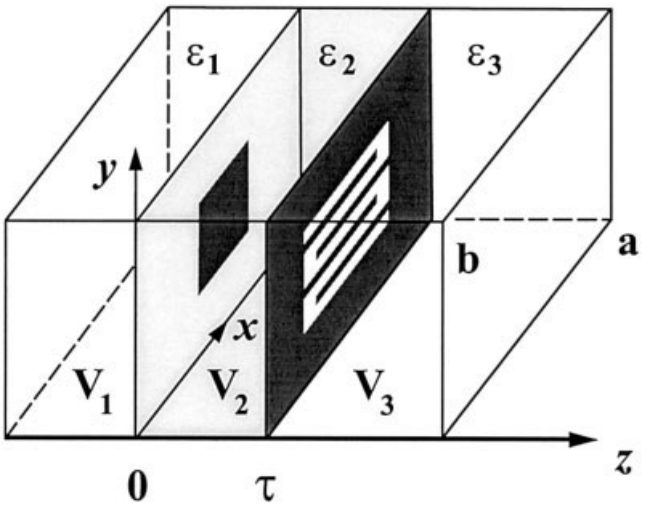

Figure 2 Interacting single-patch and meander-slot antennas in a rectangular waveguide transition

2. THEORY

The multilayered waveguide transition containing electric and magnetic-type antennas, as shown in Figure 1, is modeled by applying the integral equation formulation developed in [8, 9], resulting in the GSM of the waveguide transition. Specifically, a coupled set of integral equations for induced electric and magnetic surface current densities is obtained, and discretized via the MoM by a procedure similar to that described in [8, 9]. In this formulation, magnetic potential dyadic Green's functions of the first and second kind for a multilayered rectangular waveguide are ob-

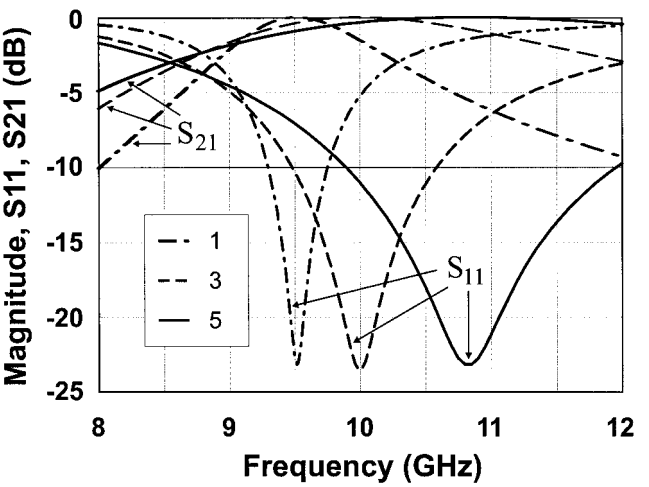

Figure 3 Magnitude of the reflection and transmission coefficients, S_{11} and S_{21}, versus frequency for the interacting meander-slot and single-patch antennas. A dash-dotted line is for the single-slot, a dashed line is for three-slot, and a solid line is for the five-slot meander antenna

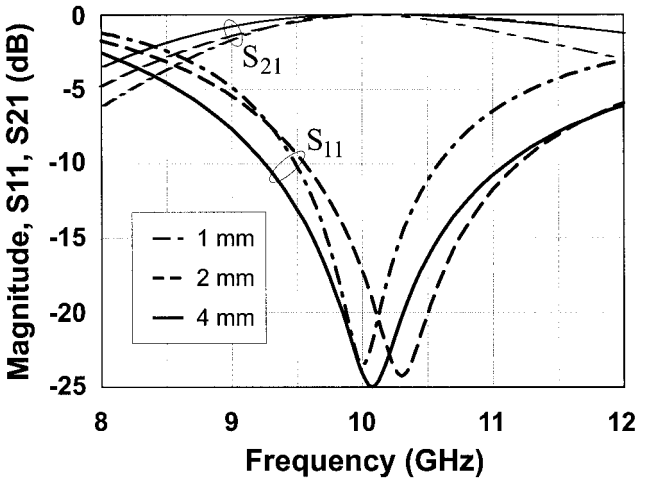

Figure 4 Magnitude of the reflection and transmission coefficients, S_{11} and S_{21}, versus frequency for different slot separation in the three-slot meander antenna coupled to a patch antenna. A dash-dotted line is for s = 1 mm, a dashed line is for s = 2 mm, and a solid line is for s = 4 mm

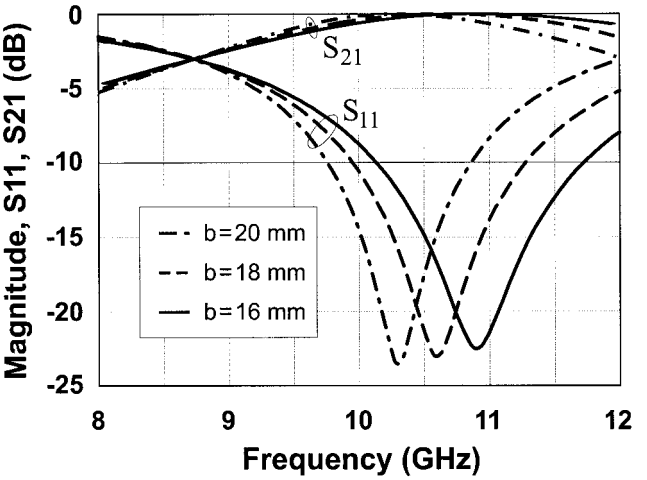

Figure 6 Magnitude of the reflection and transmission coefficients, S_{11} and S_{21}, versus frequency for the 2 × 3 interacting U-strip and three-slot meander antenna array in the waveguide transition, for a different waveguide height, b. A dash-dotted line is for b = 20 mm, a dashed line is for b = 18 mm, and a solid line is for b = 16 mm

tained, in the form of a partial eigenfunction expansion, as the solution of the system of dyadic Helmholtz equations subject to appropriate boundary and continuity conditions.

3. NUMERICAL RESULTS AND DISCUSSIONS

Scattering characteristics of meander-slot and U-slot antennas are investigated for the examples of interacting single patch and meander slot antennas, 2 × 3 interacting meander slot and patch antenna arrays, and a 3 × 3 array of interacting U-slot and U-strip antennas in overmoded waveguide transitions. The correctness of the full-wave numerical code has been checked extensively by comparison with experimental results and numerical data obtained by other methods (see [8, 9, 12], among others).

Numerical results for the S parameters of the interacting single-patch and meander-slot antennas (geometry shown in Fig. 2) in a rectangular waveguide transition operating at X-band are shown in Figure 3. The results are obtained for the following geometrical and material parameters: the rectangular waveguide is 22.86 mm × 10.16 mm, slot length in a meander configuration is 11 mm, slot width is 0.5 mm, slot separation is 1 mm, a metal patch is 2 mm × 2 mm, substrate thickness is 1 mm, $\varepsilon_1 = \varepsilon_3 = 1$, and the relative dielectric permittivity of the substrate, ε_2, is 3. The reference plane for the reflection coefficient S_{11} is at $z = 0$ (the position of the patch antenna with respect to the excitation) and the reference plane for the transmission coefficient S_{21} is at the ground plane containing meander slots ($z = \tau$). The magnitudes of the coefficients S_{22} and S_{12} are the same as those of the coefficients S_{11} and S_{21}, respectively, because of the single-mode propagation. In Figure 3, a dash-dotted line is used for the results of traditional rectangular slot antenna coupled to the patch antenna. The magnitude of the reflection coefficient (return loss) for this antenna structure has the minimum value of −23.2 dB at the resonance frequency of about 9.51 GHz. The results of the three-slot and five-slot meander antennas, coupled to the patch antenna, are

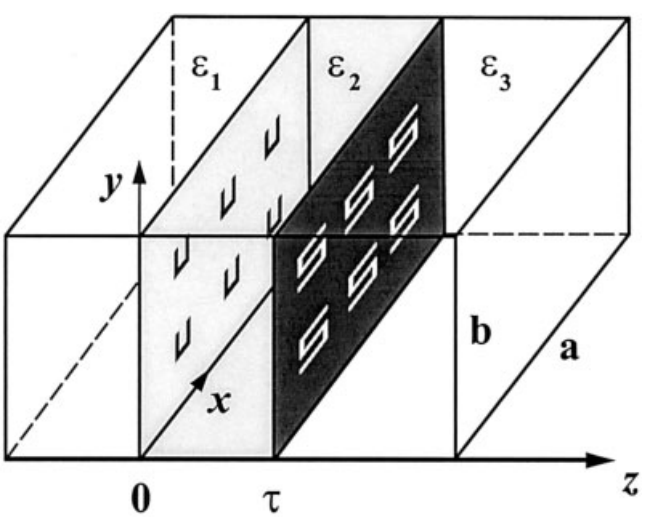

Figure 5 A 2 × 3 interacting U-strip and three-slot meander antenna array in an overmoded rectangular waveguide transition

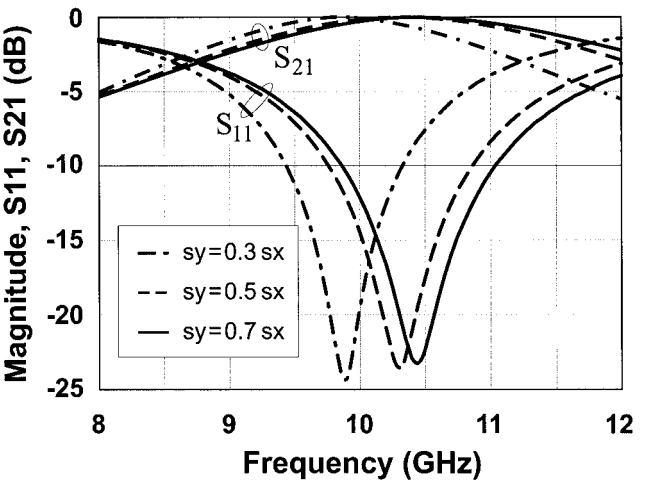

Figure 7 Magnitude of the reflection and transmission coefficients, S_{11} and S_{21}, versus frequency for the 2 × 3 interacting U-strip and three-slot meander antenna array in the waveguide transition, for different antenna separation sy in the y-direction. A dash-dotted line is for sy = 0.3, sx = 180 mil (4.572 mm), a dashed line is for sy = 0.5, sx = 300 mil (7.62 mm), and a solid line is for sy = 0.7, sx = 420 mil (10.668 mm)

depicted with dashed and solid lines, respectively. Resonance frequencies of these two antennas are shifted to higher values, namely, at 10.00 GHz and 10.85 GHz with the respective corresponding minimum values of the return loss, −23.5 dB and −23.2 dB. The percentage bandwidths of traditional rectangular slot, three-slot, and five-slot meander antennas are calculated to be 4.83%, 11.1%, and 18.8%, respectively. These increased bandwidths of the meander slot antennas demonstrate their advantage over the traditionally used rectangular slot antenna.

To evaluate the effect of the separation between slots in the three-slot meander line coupled to the patch antenna, this design parameter was successively varied, while the remaining parameters were kept the same. Figure 4 shows the calculated results for the magnitude of the reflection and transmission coefficients of this antenna structure for three different values of separation between slots. In addition to already considered slot separation of 1 mm, two other values of this parameter, 2 mm and 4 mm, were used. For the separation of 2 mm the resonance frequency is calculated to be 10.3 GHz with the frequency bandwidth of 16.0%, while the resonance frequency and bandwidth for the separation of 4 mm are obtained to be 10.08 GHz and 18.56%, respectively. Minimum return losses for the separations of 2 mm and 4 mm are obtained to be −24.3 dB and −25 dB, respectively. These results imply that an increased slot separation in the meander antenna provides a wider bandwidth while maintaining low minimum return loss at the resonance frequency.

In the next two examples, a 2 × 3 interacting U-strip and three-slot meander antenna array in an overmoded rectangular waveguide transition, as shown in Figure 5, is analyzed for operation at X-band. The first design parameter to be investigated is the waveguide height. The waveguide has 53-mm width, whereas its height is taken to be 16 mm, 18 mm, and 20 mm. The geometrical parameters for the three-slot meander antenna in the array are the same as in the first example of this section for a single unit cell. The U-strip antenna is 2 mm × 2 mm with a thickness of 0.5 mm. The dielectric has a relative permittivity of 3 with a 1-mm thickness, and the unit cells in the array are separated by a distance of 600 mil (15.24 mm) in the x direction and 300 mil (7.62 mm) in the y direction. The numerical results for the S parameters of the antenna array are shown in Figure 6. It can be seen that a decrease of the waveguide height results in an increase of the frequency bandwidth of the antenna array module. Specifically, for heights of 20 mm, 18 mm, and 16 mm, results obtained for a 10-dB return loss bandwidth were 10.68%, 12.55%, and 14.54%, respectively. Another design parameter to be investigated here is the unit cell separation in the y direction. The difference compared to the previous example is that the waveguide height is fixed to 20 mm, but the unit-cell separation in the y direction is taken to be 180 mil (4.572 mm), 300 mil (7.62 mm), and 420 mil (10.668 mm). The other geometrical and material parameters are the same as in the previous example. The numerical results for the S parameters of the antenna array are shown in Figure 7. As can be seen, an increase of the unit-cell separation in the y direction results in an increase of the frequency bandwidth of the antenna array module. Also note that the resonance frequency of the structure can be tuned by changing this design parameter.

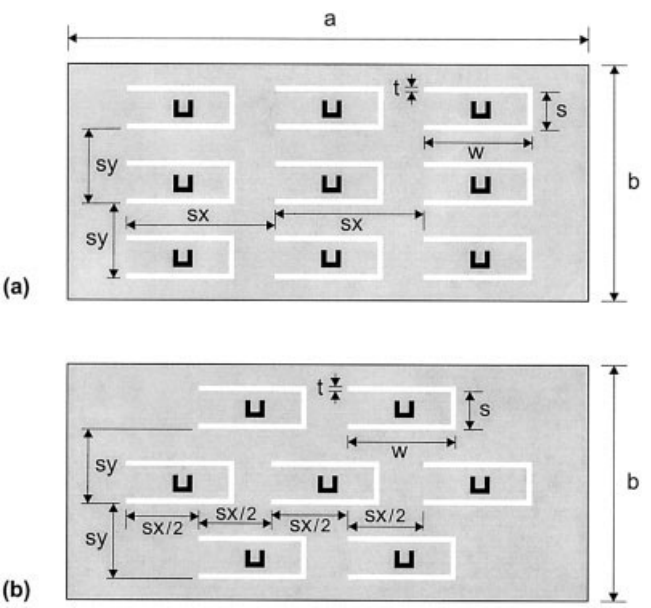

Figure 8 Geometries of the (a) 3 × 3 rectangular lattice and (b) 2 + 3 + 2 triangular lattice arrays of interacting U-slot and U-patch antennas in an overmoded rectangular waveguide transition with the following parameters: a = 53 mm, b = 24 mm, sx = 600 mil (15.24 mm), sy = 300 mil (7.62 mm), w = 11 mm, s = 4 mm, and t = 0.5 mm

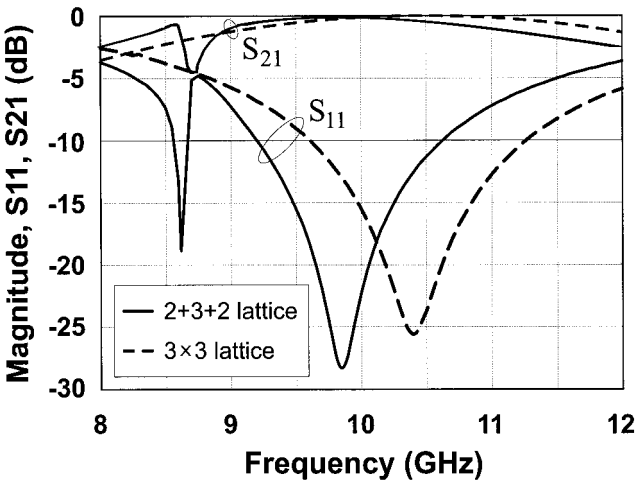

Figure 9 Magnitude of the reflection and transmission coefficients, S_{11} and S_{21}, versus frequency for the interacting U-slot and U-strip antenna arrays in the overmoded rectangular waveguide transition. A solid line is for the 2 + 3 + 2 triangular lattice and dashed line is for the 3 × 3 rectangular lattice array

In the last example, with geometry shown in Figure 8, a 3 × 3 rectangular lattice and 2 + 3 + 2 triangular lattice arrays of interacting U-slot and U-strip antennas are analyzed. Dimensions of the U-strip antennas in the array, as well as substrate thickness and permittivity, are the same as in the preceding examples. The U-slot antenna is 11 mm × 4 mm with a thickness of 0.5 mm. The unit cells in the array are separated by a distance of 600 mil (15.24 mm) in the x direction and 300 mil (7.62 mm) in the y direction, inside the waveguide which has a width of 53 mm and a height of 24 mm. The numerical results for the S parameters of the antenna arrays are shown in Figure 9. The rectangular lattice array results in a 10-dB return loss bandwidth of 15.91% at the resonance frequency of 10.4 GHz, while the triangular array had a smaller bandwidth of 14.52% at the resonance frequency of 9.85 GHz. Also note that the triangular lattice resulted in a smaller minimum return loss of −28.33 dB, compared to −25.61 dB for the rectangular lattice.

4. CONCLUSION

Numerical results for interacting single-patch and meander-slot antennas, as well as finite arrays of U-strip, U-slot, and meander slot antennas, show significant advantages in scattering characteristics in comparison to rectangular patch and slot antennas traditionally used for spatial power-combining applications. The results presented also exhibit the effect of several antenna design parameters on the frequency bandwidth and operating frequency of the system.

REFERENCES

1. M. Delisio and R. York, Quasi-optical and spatial power combining, IEEE Trans Microwave Theory Techniques Special 50th Anniversary Issue, 50 (2002), 929–936.
2. W.A. Shiroma, S.C. Bundy, S. Hollung, B.D. Bauernfeind, and Z.B. Popovic, Cascaded active and passive quasi-optical grids, IEEE Trans Microwave Theory Techniques 43 (1995), 2904–2909.
3. L.W. Epp and R.P. Smith, A generalized scattering matrix approach for analysis of quasi-optical grids and de-embedding of device parameters, IEEE Trans Microwave Theory Techniques 44 (1996), 760–769.
4. T.W. Nuteson, G.P. Monahan, M.B. Steer, K. Naishadham, J.W. Mink, K. Kojucharow, and J. Harvey, Full-wave analysis of quasi-optical structures, IEEE Trans Microwave Theory Techniques 44 (1996), 701–710.
5. A.I. Khalil, A.B. Yakovlev, and M.B. Steer, Efficient method of moments formulation for the modeling of planar conductive layers in a shielded guided-wave structure, IEEE Trans Microwave Theory Techniques 47 (1999), 1730–1736.
6. A.I. Khalil and M.B. Steer, A generalized scattering matrix method using the method of moments for electromagnetic analysis of multilayered structures in waveguide, IEEE Trans Microwave Theory Techniques 47 (1999), 2151–2157.
7. M.B. Steer, J.F. Harvey, J.W. Mink, M.N. Abdulla, C.E. Christoffersen, H.M. Gutierrez, P.L. Heron, C.W. Hicks, A.I. Khalil, U.A. Mughal, S. Nakazawa, T.W. Nuteson, J. Patwardhan, S.G. Skaggs, M.A. Summers, S. Wang, and A.B. Yakovlev, Global modeling of spatially distributed microwave and millimeter-wave systems, IEEE Trans Microwave Theory Techniques, Special Issue, 47 (1999), 830–839.
8. A.B. Yakovlev, A.I. Khalil, C.W. Hicks, A. Mortazawi, and M.B. Steer, The generalized scattering matrix of closely spaced strip and slot layers in waveguide, IEEE Trans Microwave Theory Techniques 48 (2000), 126–137.
9. A.B. Yakovlev, S. Ortiz, M. Ozkar, A. Mortazawi, and M.B. Steer, A waveguide-based aperture-coupled patch amplifier array: Full-wave system analysis and experimental validation, IEEE Trans Microwave Theory Techniques, Special Issue, 48 (2000), 2692–2699.
10. C.P. Huang, A.Z. Elsherbeni, and C.E. Smith, Analysis and design of tapered meander line antennas for mobile communications, ACES Journal 15 (2000), 159–166.
11. C.P. Huang, J.B. Chen, A.Z. Elsherbeni, and C.E. Smith, FDTD characterization of meander line antennas for RF and wireless communications, Electromagnetic Wave Monograph Series, Progress in Electromagnetic Research (PIER 24), 24 (1999), 257–277.
12. A.B. Yakovlev, S. Ortiz, M. Ozkar, A. Mortazawi, and M.B. Steer, Electric dyadic Green's functions for modeling resonance and coupling effects in waveguide-based aperture-coupled patch arrays, ACES Journal 17 (2002), 123–133.

A COMPARISON BETWEEN TWO HIGH-FREQUENCY TECHNIQUES APPLIED TO THE ANALYSIS OF ON-BOARD ANTENNAS

Olga M. Conde,[1] Francisco Sáez de Adana,[2] and Manuel F. Cátedra[2]
[1] Dep. Tec. Electrónica e Ingeniería de Sistemas y Automática
Universidad Cantabria, ETSIIT
Avda. Los Castros s/n
39005 Santander, Spain
[2] Dep. Teoría de Señal y Comunicaciones
Universidad de Alcalá de Henares
Escuela Politécnica, Campus Universitario
28806 Alcalá de Henares, Spain

Received 9 August 2002

ABSTRACT: *This paper contrasts the solutions given by the geometrical optics-uniform theory of diffraction (GO-UTD) and the physical optics-stationary phase (PO-SPM) methods when they are applied to the problem of analysis of on-board antennas. Results for both approximations are given for antennas on board a satellite mock-up. Advantages and drawbacks of both methods are shown.* © 2003 Wiley Periodicals, Inc. Microwave Opt Technol Lett 36: 415–417, 2003; Published online in Wiley InterScience (www.interscience.wiley.com). DOI 10.1002/mop.10779

Key words: *on-board antennas; diffraction theory; physical optics; high-frequency techniques; electromagnetic numerical methods*

INTRODUCTION

Several techniques can be applied to the analysis of the behaviour of on-board antennas. The research in this field strives towards the implementation of the most accurate solution with the lowest consumption of computer resources, that is, CPU time and memory. Following this line of thought, high-frequency approximations are recognised as the most suitable ones for the analysis of electrically large structures. Among this wide set of techniques, geometrical optics in combination with uniform theory of diffraction (GO-UTD) [1] has been used traditionally to solve these kinds of problems. More recently [2], the evaluation of the integral involved in physical optics making use of the stationary phase method (PO-SPM) has opened a new line of work. This paper focuses on the comparison, from a theoretical and a performance point of view, of techniques, GO-UTD and PO-SPM, when they provide solutions to a realistic problem and are confronted with measurements obtained in a satellite mock-up.

To carry out an appropriate comparison, both techniques should obviously be applied over the same structure and need to share the same geometrical representation of the geometry to be analysed. This representation is set in terms of parametric surfaces.

THEORETICAL APPROACH

For both techniques, GO-UTD and PO-SPM, the interaction between the structure and the radiation diagram of the antenna is considered, taking into account the contribution of specific points distributed along the geometry of the structure. In the case of GO-UTD, the main effects of the structure come from the contribution of the following points [1]:

- Reflection points that fulfil Snell's law between incidence and observation directions
- Diffraction points located at the edges of the geometry; at